Detection of increased vascular signal in arthritis-prone rats without joint swelling using superb microvascular imaging ultrasonography

Tatsunori Horie[a,b)], Mutsumi Nishida[a,c)], Shun Tanimura[d)], Tamotsu Kamishima[e)], Erika Tamai[e),1], Yutaka Morimura[f)], Yuka Nishibata[f)], Sakiko Masuda[f)], Daigo Nakazawa[d)], Utano Tomaru[g)], Tatsuya Atsumi[d)], Akihiro Ishizu[f)]

a) Diagnostic Center for Sonography, Hokkaido University Hospital, N-14,W-5, Kita-ku, Sapporo 060-8648, Japan

b) Department of Radiological Technology, Hokkaido University Hospital, N-14,W-5, Kita-ku, Sapporo 060-8648, Japan

c) Division of Laboratory and Transfusion Medicine, Hokkaido University Hospital, N-14,W-5, Kita-ku, Sapporo 060-8648, Japan

d) Department of Rheumatology, Endocrinology and Nephrology, Faculty of Medicine and Graduate School of Medicine, Hokkaido University, N-15, W-7, Kita-ku, Sapporo, 060-8638, Japan

e) Department of Biomedical Science and Engineering, Faculty of Health Sciences, Hokkaido University, N-12, W-5, Kita-ku, Sapporo 060-0812, Japan

f) Department of Medical Laboratory Science, Faculty of Health Sciences, Hokkaido University, N-12, W-5, Kita-ku, Sapporo 060-0812, Japan

g) Department of Pathology, Faculty of Medicine and Graduate School of Medicine, Hokkaido University, N-15, W-7, Kita-ku, Sapporo, 060-8638, Japan

1. Current affiliation: Department of Radiology, Hiroshima Prefectural Hospital, 1-5-54, Ujinakanda, Minami-ku, Hiroshima 734-8530, Japan

Corresponding author: Akihiro Ishizu, M.D., Ph. D.

Department of Medical Laboratory Science, Faculty of Health Sciences, Hokkaido University, N-12, W-5, Kita-ku, Sapporo 060-0812, Japan

Tel: +81-11-706-3385

Fax: +81-11-706-4916

E-mail: aishizu@med.hokudai.ac.jp

Abstract

This study aimed to determine whether ultrasonography (US) can detect increased vascular signal in the synovial tissue prior to overt synovitis in rheumatoid arthritis (RA). Env-pX rats that spontaneously develop RA-like synovitis were used. Ankle joints of 15 pre-morbid env-pX rats were observed with power Doppler and superb microvascular imaging (SMI) using an ultrahigh-frequency (8-24 MHz) probe. Signal values were counted as the number of pixels. The total number of vessels and vessel area in the synovial tissue were histologically evaluated. Dilated vessels were determined from the mean value of synovial vessels in three wild-type rats. In all env-pX rats, apparent synovial proliferation was not observed. However, vasodilation was evident. Only SMI values were significantly correlated with the number of dilated vessels ($r=0.585$, $p=0.022$) but not with the total number of vessels. US with SMI using ultrahigh-frequency probe can detect increased vascular signal in the synovial tissue of arthritis-prone rats.

Keywords: Animal model; Power Doppler; Rheumatoid arthritis; Superb microvascular imaging; Synovitis; Ultrasound

Introduction

Rheumatoid arthritis (RA) is a systemic autoimmune disease that causes synovitis and subsequent bone destruction. The joints affected by RA are histologically characterised by massive proliferation of synovial tissues with pronounced inflammatory cell infiltration that destroys cartilages and bones. Joint destruction by progression of synovitis reduces the quality of life in RA patients (Scott et al. 1987; Pincus et al. 1984). However, recent studies have demonstrated that early intervention in synovitis can induce persistent disease remission (Gibofsky et al. 2017). Therefore, early detection of synovitis, as well as predicting synovitis, are very important in an RA clinic.

Although the findings that precede synovitis have not been determined yet, diverse mediators of RA, such as neutrophils, monocytes, and lymphocytes, are known to be recruited into synovial tissues by blood flow (Patel et al. 2001). Gullick et al. reported the linkage of increase blood flow signals in power Doppler (PD) ultrasonography (US) to the presence of Th17 cells, the critical initiators of synovitis, in RA joints (Gullick et al. 2010). Thus, we speculated that increased

vascular signal in the synovial tissue might be detected prior to overt synovitis in RA.

US is a well-established tool for diagnosis of RA that can evaluate the activity of synovitis (Aletaha et al. 2010; Backhaus et al. 1999; Nakagomi et al. 2013; Naredo et al. 2005). The utility of US in detecting synovitis is recognised superior to visual palpation and conventional radiography (Diaz-Torne et al. 2017; Murayama et al. 2013). Grey-scale US is used to evaluate synovial thickening (Backhaus et al. 2001; Grassi et al. 1993, 2000; Iagnocco et al. 2001; Kane et al. 2003; Karim et al. 2004; Koski et al. 1990; Manger and Kalden. 1995; Naredo et al. 2003; Schmidt et al. 2004), and PD is employed to detect blood flow in affected joints. Those findings contribute to estimate disease severity (Newman et al. 1994, 1996). PD values have been shown to represent the blood vessel area in synovial tissues (Saito et al. 2016) and well reflect response to treatment (Fukae et al. 2014; Hau et al. 2002, 1999; Ribbens et al. 2003), prognosis (Ellegaard et al 2011; Koch. 1998; Salaffi et al. 2010; Scirè et al. 2009), and bone destruction (Brown et al. 2008; Fukae et al. 2014; Ikeda et al.

2013; Peluso et al. 2011). On the contrary, the usefulness of US for detection of the preceding events of synovitis remains unclear.

Basic research using small animals is necessary for developing new drugs and for evaluating their therapeutic efficacy in RA. However, there has been no method to diagnose and estimate synovitis in small animals other than histological evaluation made after sacrifice. Although some studies attempted to evaluate arthritis in small animals using an experimental ultrasonic equipment (Clavel et al.2008; Liao et al. 2016), the sensitivity to detect microvascular signalling does not appear to be satisfactory. Recently, US device with ultrahigh-frequency probes equipped with superb microvascular imaging (SMI) has been released for clinical use. SMI can eliminate motion artefacts through special image processing and sensitively depict blood flow with low velocity. Although SMI can detect microvasculature more sensitively than conventional PD in humans (Lim et al. 2018; Orlandi et al. 2017; Yokota et al. 2018; Yu et al. 2018), no trial has obtained findings prior to established synovitis in small animals using SMI and compared them with histology. In this study, we have verified whether

US with SMI using an ultrahigh-frequency (8-24 MHz) probe can detect increased vascular signal in the synovial tissue prior to overt synovitis in arthritis-prone rats.

Materials and Methods

Rats

Fifteen env-pX rats without macroscopic joint swelling (median age, 12 weeks old; range, 10 to 44 weeks old) and age-matched three wild-type rats (inbred WKAH rats) were enrolled. The env-pX rats are transgenic rats carrying the *env-pX* gene of human T-cell leukaemia virus type Ⅰ and spontaneously develop inflammatory arthritis mimicking RA with production of rheumatoid factor (RF) (Yamazaki et al. 1997). The prevalence of arthritis in env-pX rats at 6 months of age is about 80%. These rats are maintained in the room where the temperature is controlled at about 22 °C at the Institute for Animal Experimentation, Hokkaido University Graduate School of Medicine. Experiments using animals were performed in accordance with the Guidelines for the Care and Use of Laboratory Animals in Hokkaido University (permission No. 10-0029, 15-0034).

87 ***Ultrasonography***

88 Env-pX rats were sedated using inhalation anesthesia. On the left lateral
89 decubitus position, the right ankle joint was scanned with a longitudinal view by
90 US (Figure 1). To avoid interfering observation, the ankle joint was shaved before
91 US. All env-pX rats were examined either by two sonographers with 8 or 32 years
92 of experience in clinical US.

93 The ultrasonic equipment used was Canon Aplio^{TM} i800 (Canon Medical
94 Systems, Otawara, Tochigi, Japan) equipped with PLI-2004X (8-24 MHz). All
95 images were acquired at a fixed depth of 1.25 cm, and they were not magnified
96 during the observation. The frame rate and the velocity range of PD and SMI
97 were 11 frame/s, 1.6 cm/s, and 26 frame/s, 0.5 cm/s, respectively. The frequency
98 used for both PD and SMI were 12 MHz. The gain was set to the maximum value
99 of the discrepancy in which the noise disappeared. PD and SMI values were
100 determined as the number of pixels at a width of about 5 mm between the tibia
101 and the metatarsal bone. True blood flow signal was distinguished from noise as
102 a pulsatile flow during the careful observation. Because the delineation of the

boundary of the synovium was thought to be difficult, we defined that blood flow signals detected in the articular space as fine signals were blood flow signals in the synovium. Continuing signals from the proximal to the distal part right below the skin that run through horizontally were excluded as extra-articular normal blood flow signals. First, the ankle joint was visualised by identifying the tibia, tarsal bones, and metatarsal bone in grey-scale image, and sweep scan was then performed covering the entire ankle joint with PD and SMI. When the region with the most prominent blood flow signalling was detected, findings were captured at still images.

Quantitative SMI and PD values (summation of the number of coloured pixels in the joint) of US images were determined using ImageJ 1.50i (http://allpcworld.com/download-imagej-1-50i-free/) in manually defined region of interest.

Histological assessment

All env-pX rats were sacrificed immediately after completion of US scanning. Haematoxylin and eosin (HE) staining was performed for the longitudinal sections of the ankle joint. Total vessels in the synovial tissue were counted in the HE specimens. Dilated vessels were defined as vessels with area larger than 20,090 μm^2, which represented the mean plus standard deviation (SD) value of synovial vessels in three age-matched wild-type rats.

Statistical analysis

Wilcoxon-signed rank test and Mann-Whitney *U*-test were performed, and *p*-value < 0.05 was considered significant. Correlation between two continuous variables was assessed using Pearson's correlation coefficients. For statistical evaluation, SPSS version 22.0 (IBM, New York, NY, USA) and GraphPad Prism Software (ver.7.02, GraphPad Software, San Diego, CA, USA) were used.

Results

Detection of vascular signal in the synovial tissue of env-pX rats without established synovitis by US

In all env-pX rats examined (n=15), apparent synovial thickening was not detected with grey-scale US, and there was no histologically proven synovitis, such as inflammatory cell infiltration and bone erosion. PD and SMI values and total number of vessels and dilated vessels in the 15 env-pX rats are shown in Table 1. Blood flow signal was detected in 8 and 12 env-pX rats with PD and SMI, respectively. Representative histological and US findings are shown in Figure 2 (rat No. 2) and Figure 3 (rat No. 11).

Vasodilation in the synovial tissue of env-pX rats without established synovitis

Although there was no significant difference in the synovial vascular areas between env-pX rats and age-matched wild-type rats (p=0.601), many vessels with large area were found in the env-pX rats (Figure 4A). Therefore, we

149 analyzed dilated and non-dilated vessels. Although the vascular areas of non-
150 dilated vessels in the env-pX synovial tissues (8,197 ± 4,728 μm^2) were
151 comparable with those in the wild-type synovial tissues (9,665 ± 4,766 μm^2)
152 (*p*=0.059, Figure 4B), the vascular areas of dilated vessels in the env-pX synovial
153 tissues (45,610 ± 25,203 μm^2) were significantly larger than those in the wild-type
154 synovial tissues (27,481 ± 8,842) (*p*=0.013, Figure 4C). These findings suggested
155 that vasodilation occurred in the env-pX synovial tissues prior to the
156 establishment of synovitis.
157
158 **Correlation of SMI values with the numbers of dilated vessels in the**
159 **synovial tissue of env-pX rats without established synovitis**
160 SMI values were significantly larger than PD values (*p*=0.002) and
161 correlated with the number of dilated vessels (r=0.585, *p*=0.022) but not those of
162 the total vessels (*p*=0.762) in the synovial tissue (Figure 5). The number of dilated
163 vessels was not correlated with PD values (*p*=0.130).
164

Discussion

Our results demonstrate the detection of presumably increased vascular signal in the synovial tissue prior to the establishment of synovitis in arthritis-prone rats by US with SMI using an ultrahigh-frequency probe. SMI appears to be superior to PD to detect increase in synovial vascular signal. Conventional PD uses wall filter to exclude motion artifacts. However, SMI hires a new algorithm adapted to remove clutter noise by analyzing tissue motion. Microvascular blood flow with low velocity has been thought to be hardly detected by conventional PD, because low velocity in small vessels is usually buried in noise. However, SMI can successfully detect this blood flow without blooming from the vascular cavity. The blood flow velocity in the synovium has never been clarified. The lowest blood flow velocity that could be measured by PD in a basic experimental model depends on the diameter of the vessels and US machines (Cate et al. 2013). It ranged from 0.01 to 0.4 cm/s in vessels with a diameter of 150 to 2000 μm. However, the measurement of the blood flow velocity by SMI neither in a phantom model nor in the synovium has been reported. Although SMI could detect quite a

181 low-velocity blood flow, a detailed limitation of the lowest velocity detected by SMI
182 has remained unclear.

183 There are few reports on human subjects demonstrating the superiority
184 of SMI over PD in terms of detection of vascularity with improved resolution and
185 sensitivity, which may contribute to earlier detection of active inflammation and to
186 have significant impact on treatment paradigms (Yokota et al. 2018; Lim et al.
187 2018; Orlandi et al. 2017; Yu et al. 2018). To the best of our knowledge, this is
188 the first small animal study to prove similar findings with pathological correlations.
189 The implication of this work is possible application of this method to future drug
190 design for arthritides by enhancing drug efficacy.

191 Interestingly, SMI values were significantly correlated with the number
192 of dilated vessels but not the total number of vessels in the synovial tissue. This
193 suggests that dilated vessels but not all vessels contribute to the substantial
194 blood flow. Similar relationship between PD values and synovial vessels in long-
195 standing RA patients has been reported (Schmidt et al. 2000; Saito et al. 2016).
196 Koski hypothesized that this is attributed to the stage of congestion (hyperemia)

197 in the tissue rather than to the increased number of the vessel (Koshi
198 2012). Unfortunately, the regulation of synovial perfusion, namely, the exact
199 mechanism on how resistance and/or compliance of the vessels are altered at
200 the initial stage of synovitis, is largely unknown. However, when we consider that
201 the SMI signal is correlated to the perfusion, it may be a cause of synovitis.

202 There were two possible reasons for the positive blood flow signals in
203 rat numbers 6 and 12 by SMI, the joints with zero dilated vessels in pathological
204 specimens. First of all, pathological specimens did not necessarily coincide with
205 US planes. US scan was done comprehensively, and US images have a certain
206 thickness. On the contrary, the pathological specimen was made by a fixed plane
207 as the median of the ankle joints. These facts suggest that US has higher
208 sensitivity to detect blood flow signals than one slice of a pathological specimen.
209 The second possibility was that the signal detected by SMI might capture normal
210 vessels that were not in the joints.

211 A limitation of this study is that cross-sectional images obtained by US
212 do not necessarily coincide with histological specimens. However, we observed

213 relatively small joints, and US images had certain thickness, the 24 MHz matrix
214 array probe that we used had presumably less than 5 mm beam width in one US
215 image plane (no disclosure of specifications of US beam forming) so that US
216 images obtained by our study nearly covered the ankle joints of rats.

217 Another limitation is a lack of follow-up study. To compare the US
218 findings with histology, we had to sacrifice rats immediately after US scanning.
219 Prospective studies are needed to confirm the association between initial
220 increase in synovial blood flow detected by US and future development of
221 synovitis in rats. In our pilot study using env-pX rats, blood flow was initially
222 detected in the synovium, and synovial thickening followed 2 weeks later
223 (unpublished data). We believe that increase in synovial blood flow induced by
224 vasodilation triggers the initiation of synovitis.

225 In addition, the usage of a single animal model is also a critical limitation
226 in this study. Although env-pX rats are suitable models of RA (Yamazaki et al.
227 1997), reproducibility of results should be determined using other RA models.

228

Conclusion

Despite the limitations, our study demonstrated that SMI can detect increase in synovial blood flow prior to overt synovitis and gave us a motivation to perform this experiment on human joints. Prediction and early diagnosis of synovitis are inevitable to achieve complete and persistent remission of RA.

Acknowledgements

We are grateful to Mr. Hiraku Shida (Tonan Hospital, Sapporo, Japan) for technical assistance.

References

Aletaha D, Neogi T, Silman AJ, Funovits J, Felson DT, Bingham CO 3rd, Birnbaum NS, Burmester GR, Bykerk VP, Cohen MD, Combe B, Costenbader KH, Dougados M, Emery P, Ferraccioli G, Hazes JM, Hobbs K, Huizinga TW, Kavanaugh A, Kay J, Kvien TK, Laing T, Mease P, Ménard HA, Moreland LW, Naden RL, Pincus T, Smolen JS, Stanislawska-Biernat E, Symmons D, Tak PP, Upchurch KS, Vencovský J, Wolfe F, Hawker G. 2010 rheumatoid arthritis classification criteria: an American College of Rheumatology/European League Against Rheumatism collaborative initiative. Ann Rheum Dis 2010;69:1580–8.

Backhaus M, Kamradt T, Sandrock D, Loreck D, Fritz J, Wolf KJ, Raber H, Hamm B, Burmester GR, Bollow M. Arthritis of the finger joints: a comprehensive approach comparing conventional radiography, scintigraphy, ultrasound, and contrast-enhanced magnetic resonance imaging. Arthritis Rheum 1999;42:1232–45.

255

256 Backhaus M, Burmester GR, Gerber T, Grassi W, Machold KP, Swen WA,
257 Wakefield RJ, Manger B; Working Group for Musculoskeletal Ultrasound in the
258 EULAR Standing Committee on International Clinical Studies including
259 Therapeutic Trials. Guidelines for musculoskeletal ultrasound in rheumatology.
260 Ann Rheum Dis 2001;60:641–9.

261

262 Brown AK, Conaghan PG, Karim Z, Quinn MA, Ikeda K, Peterfy CG, Hensor E,
263 Wakefield RJ, O'Connor PJ, Emery P. An explanation for the apparent
264 dissociation between clinical remission and continued structural deterioration in
265 rheumatoid arthritis. Arthritis Rheum 2008;58:2958–67.

266

267 Cate TD, Luime JJ, van der Ven M, Hazes JMW, Kooiman K, de Jong N, Bosch
268 GJ. Very different performance of power Doppler modalities of several ultrasound

machines ascertained by a microvessel flow phantom. Arthritis Res Ther 2013;15:R162.

Clavel G, Marchiol-Fournigault C, Renault G, Boissier MC, Fradelizi D, Bessis N. Ultrasound and Doppler micro-imaging in a model of rheumatoid arthritis in mice. Ann Rheum Dis 2008;67:1765–72.

Diaz-Torne C, Moragues C, Toniolol E, Geli C, Castellví I, Moya P, Gich I, Llobet JM. Impact of ultrasonography on treatment decision in rheumatoid arthritis: the IMPULSAR study. Rheumatol Int 2017;37:891–6.

Ellegaard K, Christensen R, Torp-Pedersen S, Terslev L, Holm CC, Kønig MJ, Jensen PS, Danneskiold-Samsøe B, Bliddal H. Ultrasound Doppler measurements predict success of treatment with anti-TNF-α drug in

283 patients with rheumatoid arthritis: a prospective cohort study. Rheumatology
284 2011;50:506–12.

285

286 Fukae J, Tanimura K, Atsumi T, Koike T. Sonographic synovial vascularity of
287 synovitis in rheumatoid arthritis. Rheumatology 2014;53:586–91.

288

289 Gibofsky A, Yazici Y. Treatment of rheumatoid arthritis: strategies for achieving
290 optimal outcomes. Rheumatol Int 2017;37:891–6.

291

292 Grassi W, Tittarelli E, Pirani O, Avaltroni D, Cervini C. Ultrasound examination of
293 metacarpophalangeal joints in rheumatoid arthritis. Scand J Rheumatol.
294 1993;22:243–7.

295

296 Grassi W, Filippucci E, Farina A, Cervini C. Sonographic imaging of tendons.
297 Arthritis Rheum 2000;43:969.

298

299 Gullick NJ, Evans HG, Church LD, Jayaraj DM, Filer A, Kirkham BW, Taams LS.
300 Linking power Doppler ultrasound to the presence of Th17 cells in the rheumatoid
301 arthritis joint. PLoS One 2010;5:e12516.

302

303 Hau M, Schultz H, Tony HP, Keberle M, Jahns R, Haerten R, Jenett M. Evaluation
304 of pannus and vascularization of the metacarpophalangeal and proximal
305 interphalangeal joints in rheumatoid arthritis by high-resolution ultrasound
306 (multidimensional linear array). Arthritis Rheum 1999;42:2303–8.

307

308 Hau M, Kneitz C, Tony HP, Keberle M, Jahns R, Jenett M. High resolution
309 ultrasound detects a decrease in pannus vascularisation of small finger joints in

310 patients with rheumatoid arthritis receiving treatment with soluble tumour
311 necrosis factor alpha receptor (etanercept). Ann Rheum Dis 2002;61:55–8.

312

313 Iagnocco A, Coari G, Palombi G, Valesini G. Sonography in the study of
314 metatarsalgia. J Rheumatol 2001;28:1338–40.

315

316 Ikeda K, Nakagomi D, Sanayama Y, Yamagata M, Okubo A, Iwamoto T,
317 Kawashima H, Takahashi K, Nakajima H. Correlation of radiographic progression
318 with the cumulative activity of synovitis estimated by power Doppler ultrasound
319 in rheumatoid arthritis: difference between patients treated with methotrexate and
320 those treated with biological agents. J Rheumatol 2013;40:1967–76.

321

322 Kane D, Balint P V, Sturrock RD. Ultrasonography is superior to clinical
323 examination in the detection and localization of knee joint effusion in rheumatoid
324 arthritis. J Rheumatol. 2003;30:966–71.

325

326 Karim Z, Wakefield RJ, Quinn M, Conaghan PG, Brown AK, Veale DJ, O'Connor
327 P, Reece R, Emery P. Validation and reproducibility of ultrasonography in the
328 detection of synovitis in the knee: A comparison with arthroscopy and clinical
329 examination. Arthritis Rheum 2004;50:387–94.

330

331 Koch AE. Review: angiogenesis: implications for rheumatoid arthritis. Arthritis
332 Rheum 1998;41:951–62.

333

334 Koski JM, Anttila P, Hämäläinen M, Isomäki H. Hip joint ultrasonography:
335 correlation with intra-articular effusion and synovitis. Br J Rheumatol.
336 1990;29:189–92.

337

338 Koshi JM. Doppler imaging and histology of the synovium. J Rheumatol
339 2012;39:452-3.

340

341 Liao AH, Chung HY, Chen WS, Yeh MK. Efficacy of combined ultrasound-and-
342 microbubbles-mediated diclofenac gel delivery to enhance transdermal
343 permeation in adjuvant-induced rheumatoid arthritis in the rat. Ultrasound Med
344 Biol 2016;42:1976–85.

345

346 Lim AKP, Satchithananda K, Dick EA, Abraham S, Cosgrove DO. Microflow
347 imaging: New Doppler technology to detect low-grade inflammation in patients
348 with arthritis. Eur Radiol 2018;28:1046–53.

349

350 Manger B, Kalden JR. Joint and connective tissue ultrasonography--a
351 rheumatologic bedside procedure? A German experience. Arthritis Rheum
352 1995;38:736–42.

353

354 Murayama G, Ogasawara M, Nemoto T, Yamada Y, Ando S, Minowa K, Kon T,
355 Tada K, Matsushita M, Yamaji K, Tamura N, Takasaki Y. Clinical miscount of
356 involved joints denotes the need for ultrasound complementation in usual practice
357 for patients with rheumatoid arthritis. Clin Exp Rheumatol 2013;31:506–14.

358

Nakagomi D, Ikeda K, Okubo A, Iwamoto T, Sanayama Y, Takahashi K, Yamagata M, Takatori H, Suzuki K, Takabayashi K, Nakajima H. Ultrasound can improve the accuracy of the 2010 American College of Rheumatology/European League against rheumatism classification criteria for rheumatoid arthritis to predict the requirement for methotrexate treatment. Arthritis Rheum 2013;65:890–8.

Naredo E, Iagnocco A, Valesini G, Uson J, Beneyto P, Crespo M. Ultrasonographic study of painful shoulder. Ann Rheum Dis. 2003;62:1026–7.

Naredo E, Bonilla G, Gamero F, Uson J, Carmona L, Laffon A. Assessment of inflammatory activity in rheumatoid arthritis: a comparative study of clinical evaluation with grey scale and power Doppler ultrasonography. Ann Rheum Dis 2005;64:375–81.

374 Newman JS, Adler RS, Bude RO, Rubin JM. Detection of soft-tissue hyperemia:
375 Value of power Doppler sonography. Am J Roentgenol 1994;163:385–9.

376

377 Newman JS, Laing TJ, McCarthy CJ, Adler RS. Power Doppler sonography of
378 synovitis: assessment of therapeutic response--preliminary observations.
379 Radiology 1996;198:582–4.

380

381 Orlandi D, Gitto S, Perugin Bernardi S, Corazza A, Flaviis L, Silvestri E, Cimmino
382 MA, Sconfienza LM. Advanced power Doppler technique increases synovial
383 vascularity detection in patients with rheumatoid arthritis. Ultrasound Med Biol
384 2017;43:1880–7.

385

386 Patel DD, Haynes BF. Leukocyte homing to synovium. Curr Dir Autoimmun.
387 2001;3:133–67.

Peluso G, Michelutti A, Bosello S, Gremese E, Tolusso B, Ferraccioli G. Clinical and ultrasonographic remission determines different chances of relapse in early and long standing rheumatoid arthritis. Ann Rheum Dis 2011;70:172–5.

Pincus T, Callahan LF, Sale WG, Brooks AL, Payne LE, Vaughn WK. Severe functional declines, work disability, and increased mortality in seventy-five rheumatoid arthritis patients studied over nine years. Arthritis Rheum 1984;27:864–72.

Ribbens C, André B, Marcelis S, Kaye O, Mathy L, Bonnet V, Beckers C, Malaise MG. Rheumatoid hand joint synovitis: gray-scale and power Doppler US quantifications following anti-tumor necrosis factor-alpha treatment: pilot study. Radiology 2003;229:562–9.

402

403 Saito K, Abe A, Kamishima T, Ishikawa H, Wakaki K, Ishizu A. Relationship
404 between power Doppler grade and the pathological blood vessel features in long-
405 standing rheumatoid arthritis. Rheumatol Int 2016;36:1689–90.

406

407 Salaffi F, Ciapetti A, Gasparini S, Carotti M, Filippucci E, Grassi W. A clinical
408 prediction rule combining routine assessment and power Doppler
409 ultrasonography for predicting progression to rheumatoid arthritis from early-
410 onset undifferentiated arthritis. Clin Exp Rheumatol 2010;28:686–94.

411

412 Schmidt WA, Völker L, Zacher J, Schläfke M, Ruhnke M, Gromnica-Ihle E. Colour
413 Doppler ultrasonography to detect pannus in knee joint synovitis. Clin Exp
414 Rheumatol 2000;18:439-44.

415

416 Schmidt WA, Schmidt H, Schicke B, Gromnica-Ihle E. Standard reference values
417 for musculoskeletal ultrasonography. Ann Rheum Dis 2004;63:988–94.

418

419 Scirè CA, Montecucco C, Codullo V, Epis O, Todoerti M, Caporali R.
420 Ultrasonographic evaluation of joint involvement in early rheumatoid arthritis in
421 clinical remission: power Doppler signal predicts short-term relapse.
422 Rheumatology 2009;48:1092–7.

423

424 Scott DL, Symmons DP, Coulton BL, Popert AJ. Long-term outcome of treating
425 rheumatoid arthritis: results after 20 years. Lancet 1987;16:1108–11.

426

427 Yamazaki H, Ikeda H, Ishizu A, Nakamaru Y, Sugaya T, Kikuchi K, Yamada S,
428 Wakisaka A, Kasai N, Koike T, Hatanaka M, Yoshiki T. A wide spectrum of

collagen vascular and autoimmune diseases in transgenic rats carrying the env-pX gene of human T lymphocyte virus type I. Int Immunol 1997;9:339–46.

Yokota K, Tsuzuki Wada T, Akiyama Y, Mimura T. Detection of synovial inflammation in rheumatic diseases using superb microvascular imaging: Comparison with conventional power Doppler imaging. Mod Rheumatol 2018;28:327–33.

Yu X, Li Z, Ren M, Xi J, Wu J, Ji Y. Superb microvascular imaging (SMI) for evaluating hand joint lesions in patients with rheumatoid arthritis in clinical remission. Rheumatol Int. 2018;38:1885–90.

441 **Figure Legends**

442 **Fig. 1. Rat ankle joint**

443 A: Rat lower leg.

444 B: Loupe view of the haematoxylin and eosin staining section.

445 C: X-ray image showing anatomical orientation of the joint.

446 D: Grey-scale ultrasound scan showing the ankle joint with the tibia, tarsal bones,

447 and metatarsal bone.

448 T: Tibia, M: Metatarsal bone.

449

450 **Fig. 2. Representative findings (rat No. 2)**

451 The tibia, tarsal bones, and metatarsal bone in the ankle joint are seen in the

452 sagittal plane of the haematoxylin and eosin specimen (×20) (A), grey-scale

453 image (B), PD image (C), and SMI (D). A: Only one dilated vessel is seen in the

454 specimen (yellow arrow head) B: Grey-scale image shows no thickening of the

455 synovium. C: PD image shows no blood flow. D: SMI shows no blood flow.

456 PD, power Doppler; SMI, superb microvascular imaging

Fig. 3. Representative findings (rat No. 11)

The tibia, tarsal bones, and metatarsal bone in the ankle joint are seen in sagittal view of the haematoxylin and eosin specimen (×20) (A), grey-scale image (B), PD image (C), and SMI (D). A: Three dilated vessels are seen in the specimen (yellow arrow heads). B: Grey-scale image shows no thickening of the synovium. C: PD image shows blood flow (arrows). D: SMI shows blood flow (arrows). SMI depicted greater pixel counts (4,570) than PD (2,865).

PD, power Doppler; SMI, superb microvascular imaging

Fig. 4. Comparison of vessel areas in the synovial tissues between wild-type and env-pX rats.

(A) Comparison of areas of all vessels in the synovial tissues between wild-type rats (55 vessels in 3 rats) and env-pX rats (153 vessels in 15 rats). (B) Comparison of areas of non-dilated vessels in the synovial tissues between wild-type rats (48 vessels in 3 rats) and env-pX rats (123 vessels in 15 rats). (C)

472 Comparison of areas of dilated vessels in the synovial tissues between wild-type
473 rats (7 vessels in 3 rats) and env-pX rats (30 vessels in 15 rats).
474
475 **Fig. 5. Correlation between PD and SMI values and numbers of total and**
476 **dilated vessels**
477 SMI values were significantly correlated with the numbers of dilated vessels
478 (r=0.585, *p*=0.022) but not with the total number of vessels (*p*=0.762) in the
479 synovial tissue. The numbers of dilated vessels were not correlated with PD
480 values (*p*=0.130).
481 PD, power Doppler; SMI, superb microvascular imaging

Table 1. PD and SMI values and numbers of total and dilated vessels in env-pX rats

Rat number (n=15)	PD values [pixels]	SMI values [pixels]	Number of total vessels	Number of dilated vessels[a]
1	0	1,504	5	1
2	0	0	5	1
3	0	0	8	2
4	0	1,780	11	2
5	0	222	26	2
6	518	2,094	16	0
7	0	2,384	8	3
8	756	3,637	8	5
9	0	0	3	0
10	807	1,793	9	2
11	2,865	4,570	14	3
12	994	1,291	5	0
13	2,507	4,368	12	4
14	813	4,054	9	2
15	483	954	14	3

a) Dilated vessels were defined as vessels with area larger than 20,090 μm^2, which represented the mean + SD value of wild-type synovial vessels.

PD, power Doppler; SMI, superb microvascular imaging

Figure 1

A

B

C

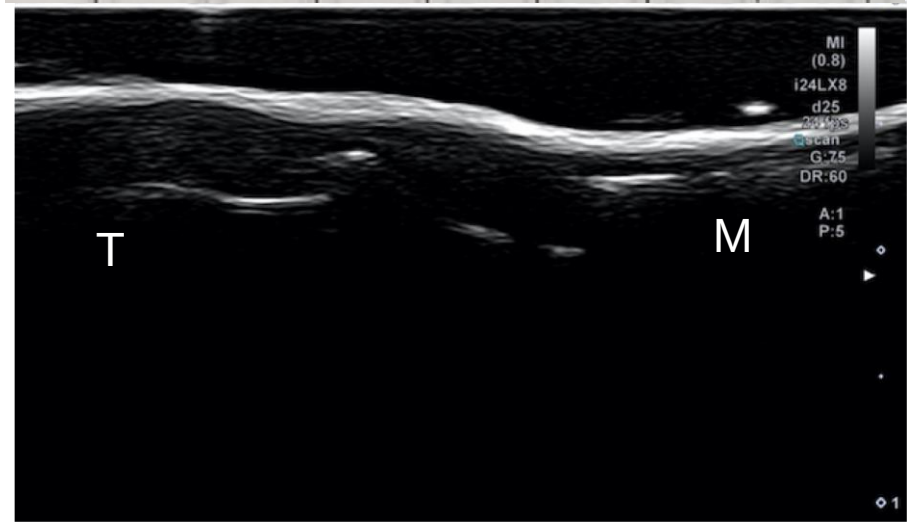

D

Figure 2

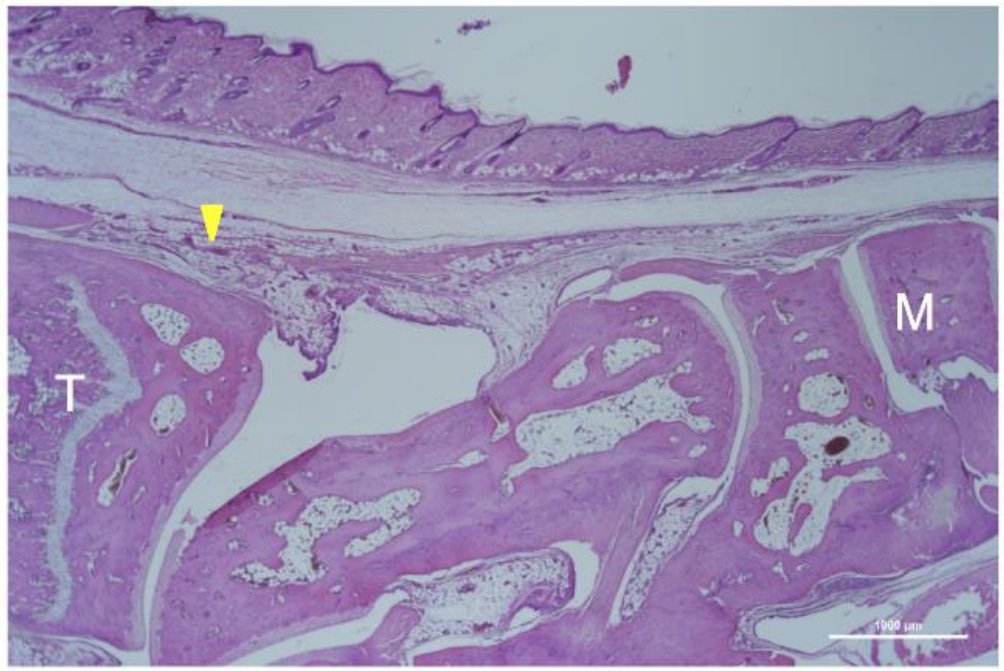

A

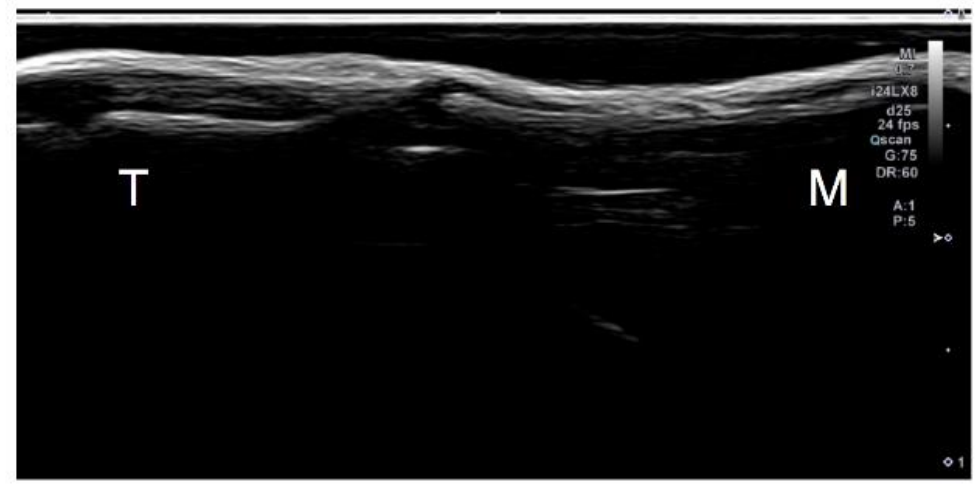

B

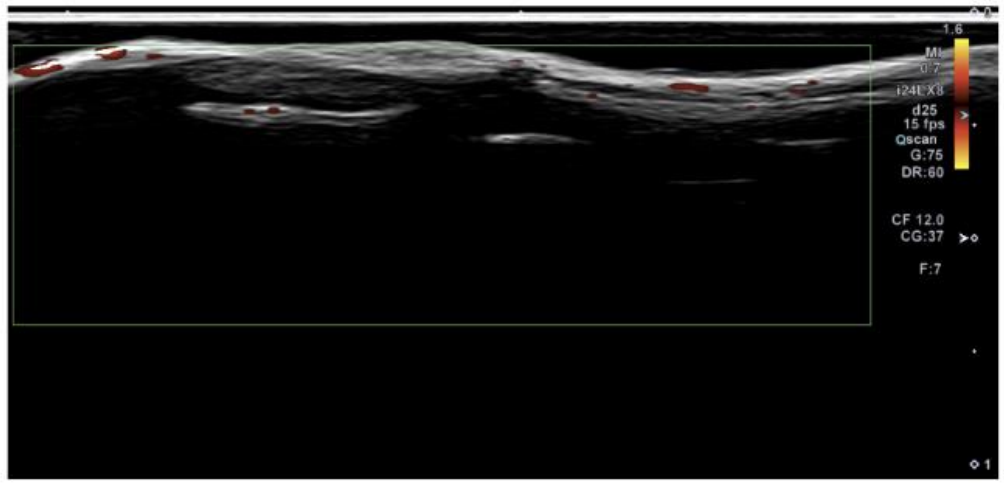

C

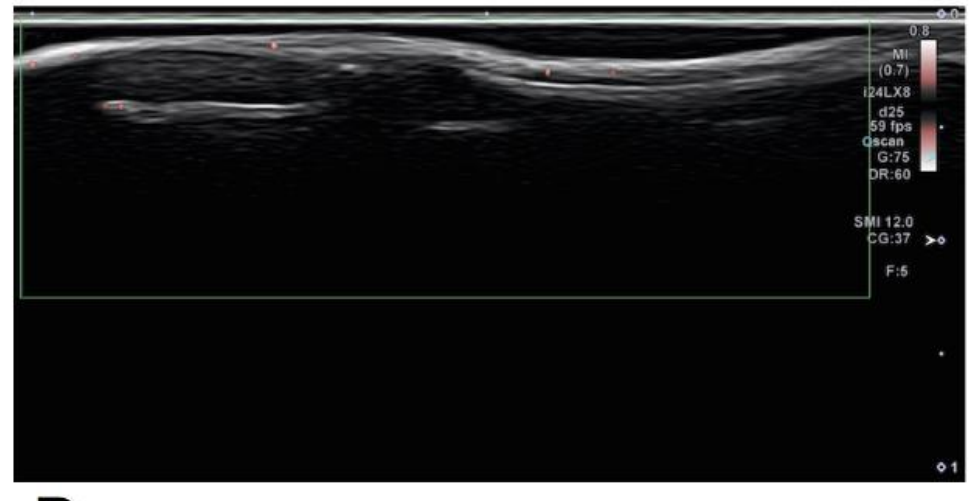

D

Figure 3

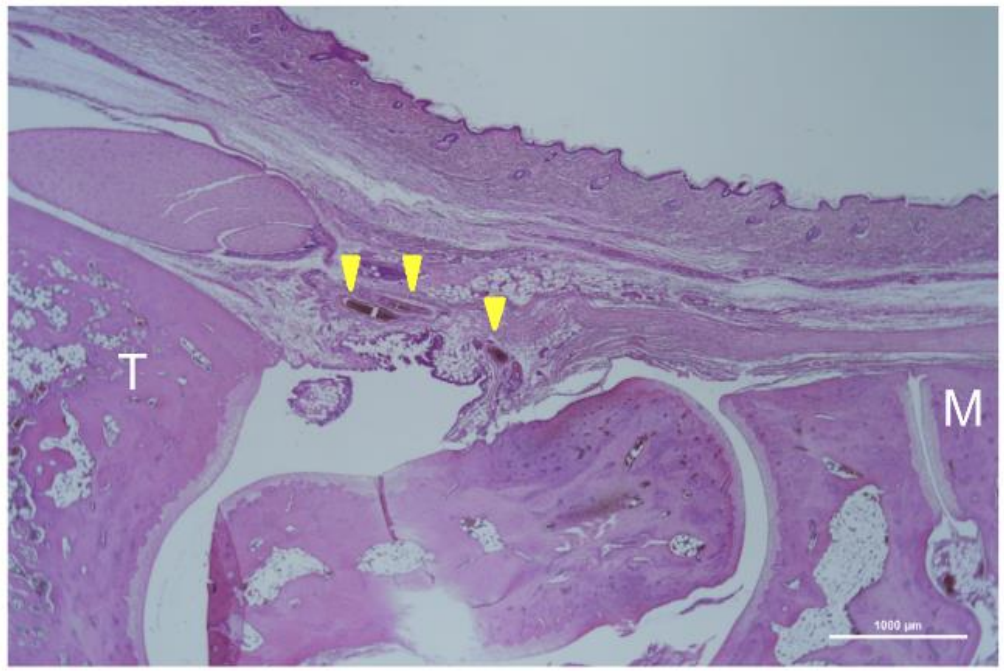

A

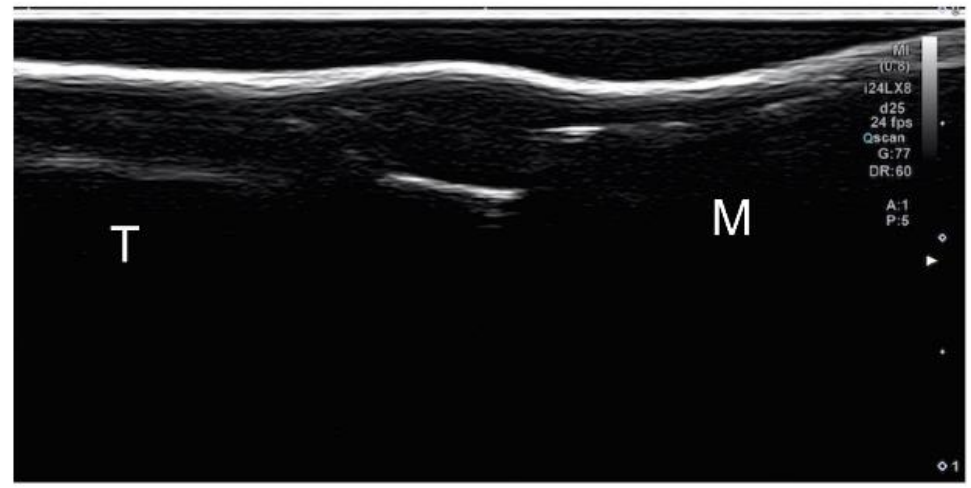

B

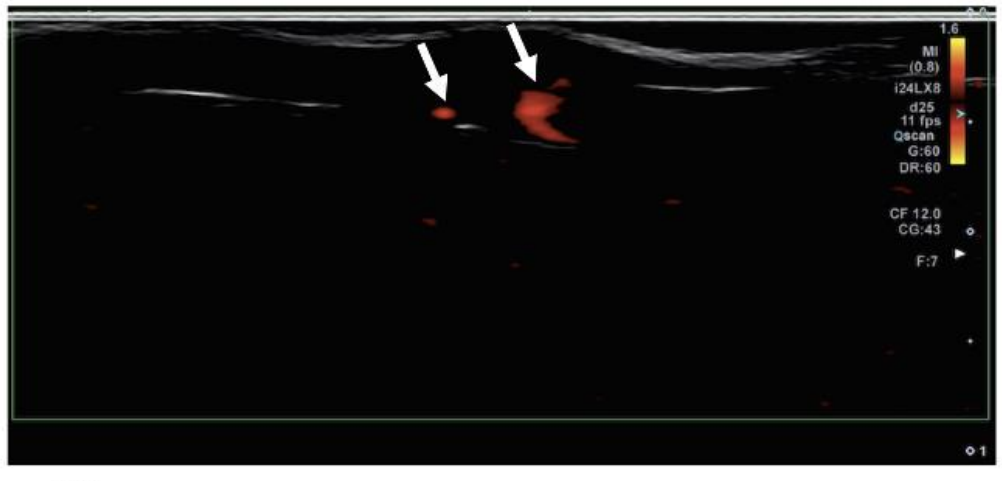

C

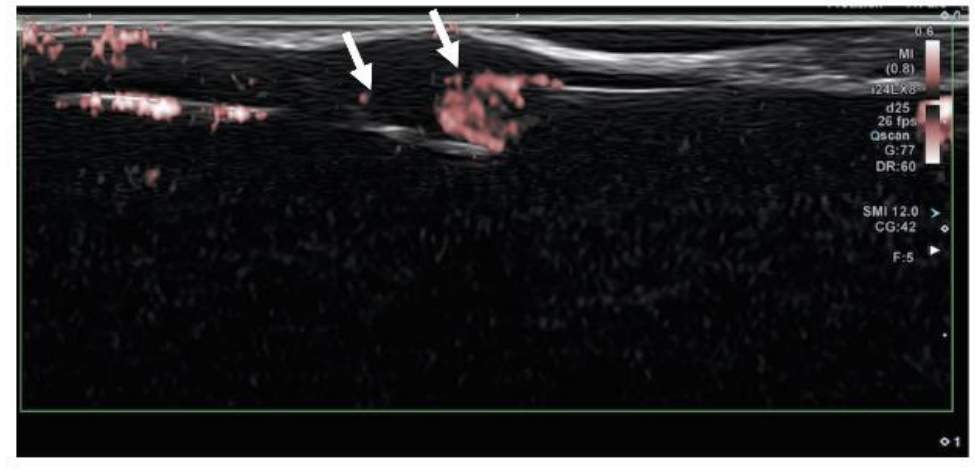

D

Figure 4

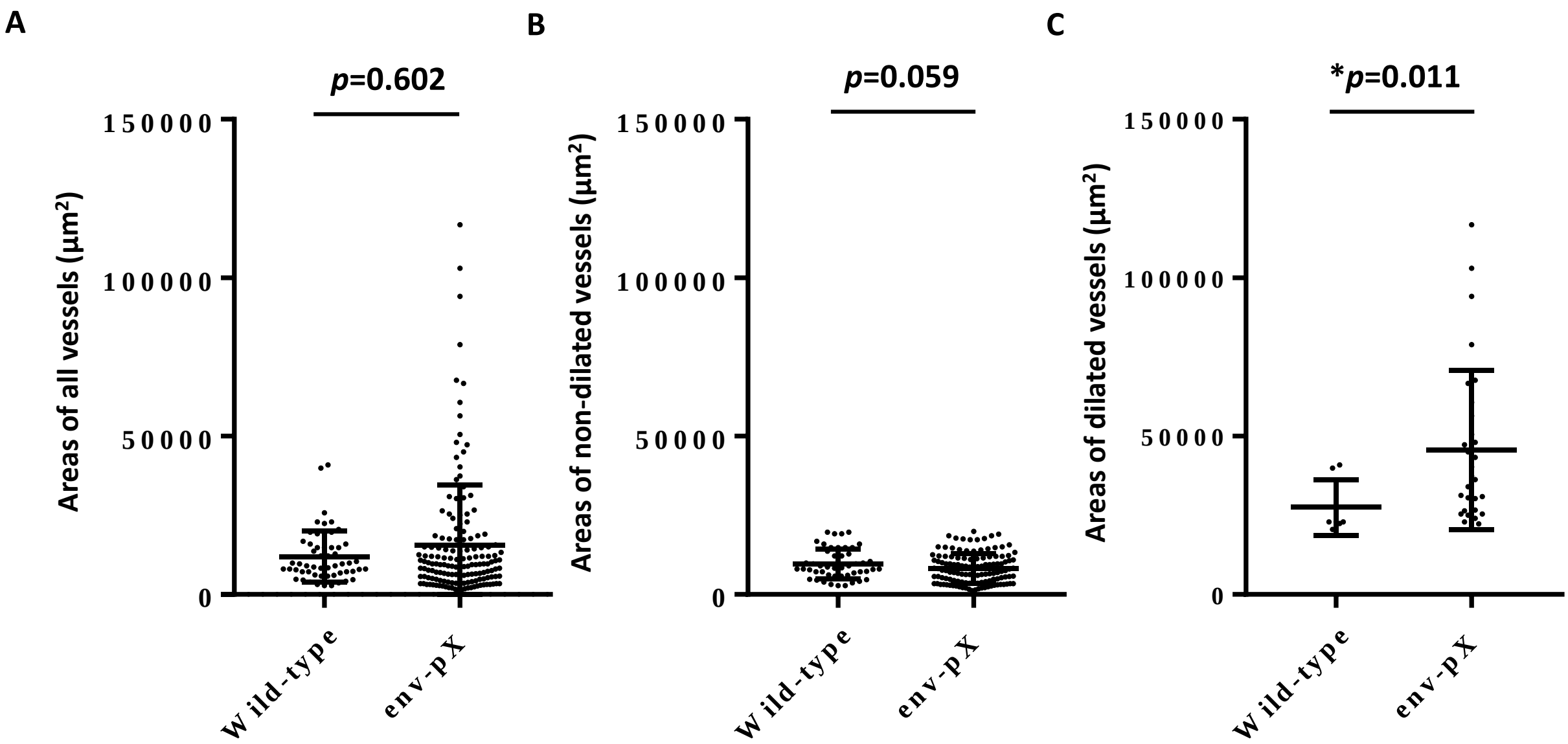
A
p=0.602
Areas of all vessels (µm²)
150000
100000
50000
0
Wild-type
env-pX
B
p=0.059
Areas of non-dilated vessels (µm²)
150000
100000
50000
0
Wild-type
env-pX
C
*p=0.011
Areas of dilated vessels (µm²)
150000
100000
50000
0
Wild-type
env-pX

Figure 5

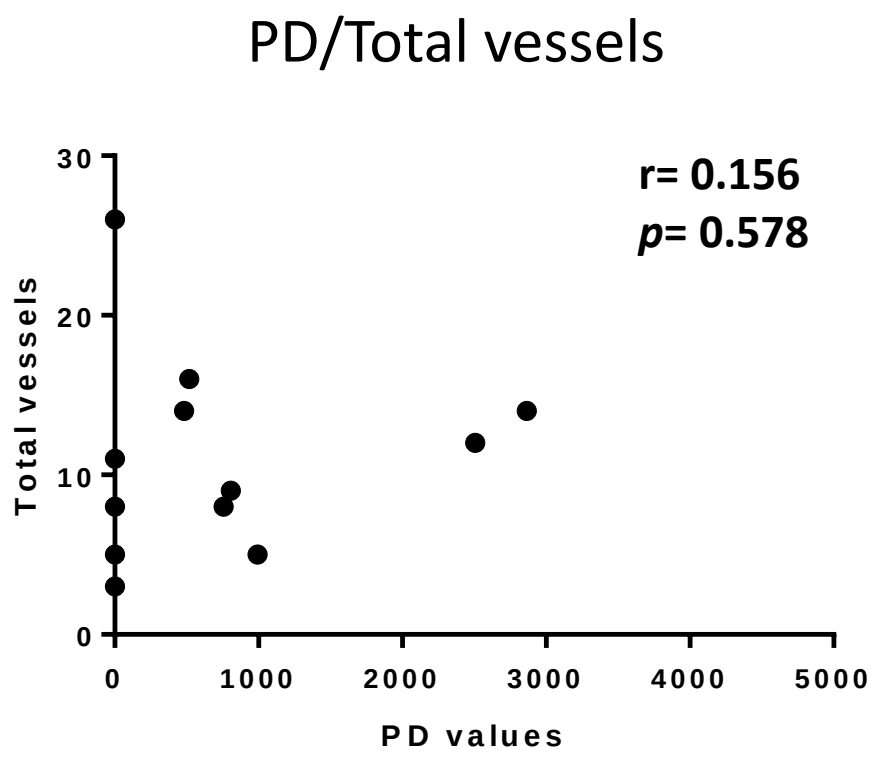
PD/Total vessels
r= 0.156
p= 0.578
Total vessels
PD values
0
10
20
30
0
1000
2000
3000
4000
5000

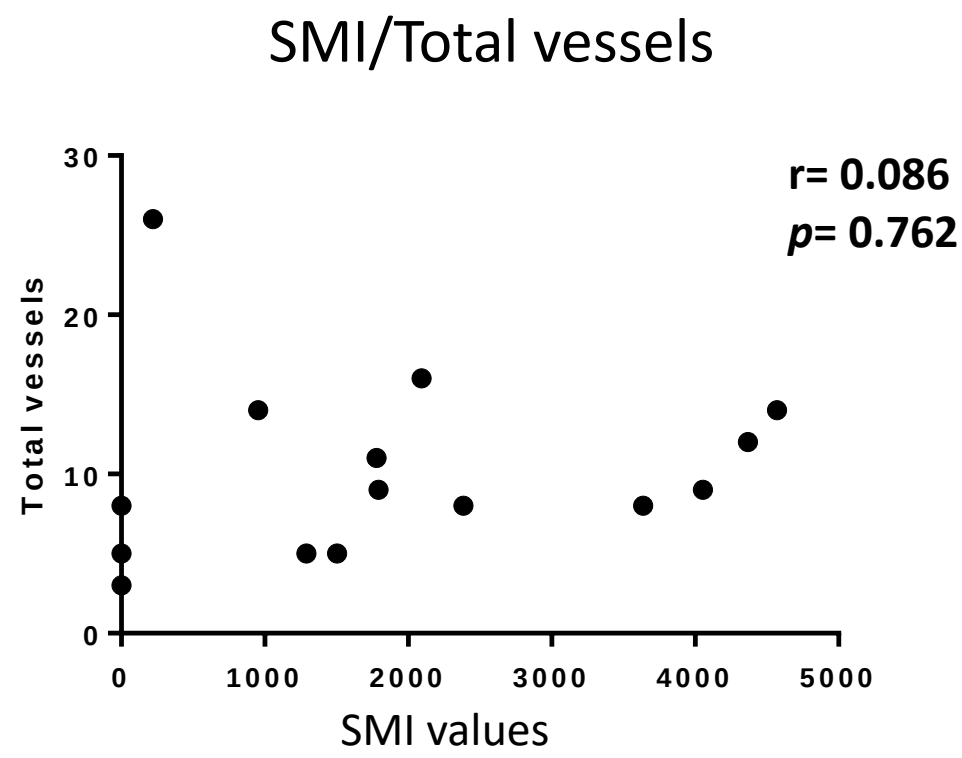
SMI/Total vessels
r= 0.086
p= 0.762
Total vessels
SMI values
0
10
20
30
0
1000
2000
3000
4000
5000

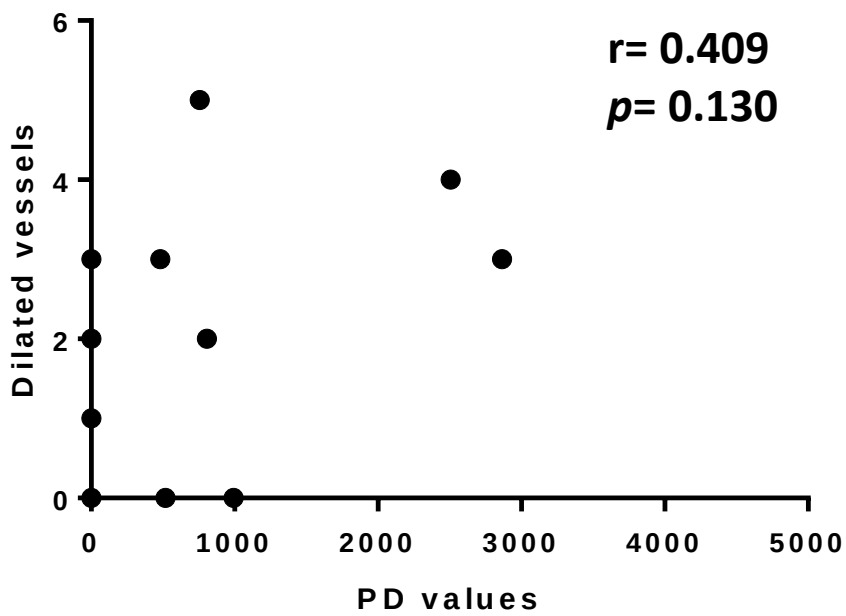
PD/Dilated vessels
r= 0.409
p= 0.130
Dilated vessels
PD values
0
2
4
6
0
1000
2000
3000
4000
5000

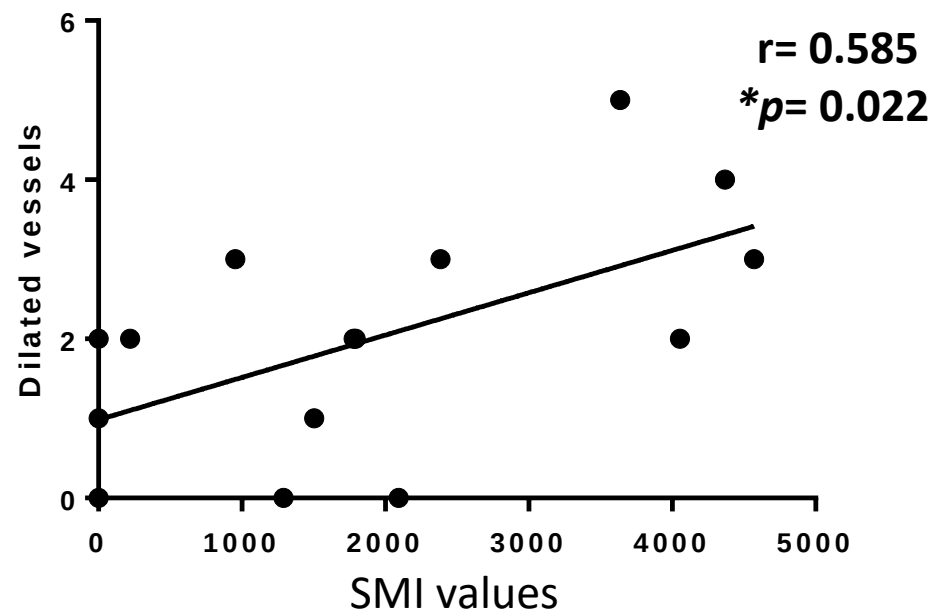
SMI/Dilated vessels
r= 0.585
*p= 0.022
Dilated vessels
SMI values
0
2
4
6
0
1000
2000
3000
4000
5000